JOURNAL OF ENGINEERING SCIENCES

Volume 8, Issue 2 (2021)

Onysko O., Karabegović I., Dašić P, Penderetskyi M., Melnyk O. (2021). The stress state of compact mechatronic satellites of a cycloidal reducer. Journal of Engineering Sciences, Vol. 8(2), pp. D12-D17, doi: 10.21272/jes.2021.8(2).d3

The Stress State of Compact Mechatronic Satellites of a Cycloidal Reducer

Onysko O.[1*[0000-0002-6543-9554]], Karabegović I.[2[0000-0001-9440-4441]], Dašić P.[3,4[0000-0002-9242-274X]], Penderetskyi M.[1], Melnyk O.[1]

[1] Ivano-Frankivsk National Technical University of Oil and Gas, 15, Karpatska St., 76000 Ivano-Frankivsk, Ukraine;
[2] Academy of Sciences and Arts of Bosnia and Herzegovina, 7, Bistrik St., 71000 Sarajevo, Bosnia and Herzegovina;
[3] SaTCIP Publisher Ltd., 36210 Vrnjačka Banja, Serbia;
[4] Faculty of Information Technology and Engineering (FITI), 11070 Novi Beograd, Serbia

Article info:
Submitted: September 3, 2021
Accepted for publication: December 6, 2021
Available online: December 11, 2021

***Corresponding email:**
onysko.oleg@gmail.com

Abstract. One of the urgent problems of mechanics is to design a lightweight, compact and precise reducer with high efficiency since it is an essential part of the robot actuators. The manufacture of modern toy robots made as Pet-models requires highly efficient and very compact drives. A topical part of the drive is the cycloidal reducer required to provide the torque appropriate for the effective movement of the toy. The article proposes a three-dimensional model of a cycloidal reducer designed for a four-legged walking robot toy. The outer diameter of the reducer is 56 mm. If its most significant parts are plastic, the weight does not exceed more than 0.2 kg. The obtained results of the analysis of stresses arising between the disk and the rollers indicate the complete suitability of the selected materials of polyamide and steel on their mechanical characteristics for use in the reducer of the robot actuator.

Keywords: slow speed shaft roller, cycloidal disk, bearing, finite end method.

1 Introduction

Nowadays, legged robots are becoming very popular among different groups of modern human society. They belong to one of these groups, and a pet simulated robot can be trendy shortly. Most of the natural pets are small: dogs and cats. But they are brisk, so the pet simulated robots must be prompt too. Therefore, robotics engineering deals with those types of toys and has to solve many problems of strength materials and compact and lightweight actuators for ones. One of the complex problems is to design an ultra-lightweight and high-efficiency compact cycloidal reducer.

2 Literature Review

The cycloidal planetary transmissions are widely used in mechanical efficiency automatic wheels and multi-legged platforms [1].

The article [2] describes a humanoid robotics platform and describes the design criteria, hardware, software framework, and experimental testing of the platform. But it does not offer the reducer design.

The paper [3] shows the general trends in the engines of humanoid robots, which of course, involve the use of structures of light drives.

In [4], authors developed a highly efficient compact cycloidal gearbox for legged robots, which uses needle roller bearings in all parts where there is contact during the power transfer process inside the gearbox, which significantly improves efficiency compared to a cycloidal gearbox using free rollers. The paper proposes the sub-carrier structure that distributes the load and allows the cycloidal gear to respond reliably to shocks that may occur while the robot is moving on its feet. But it weighs 766 g, so it can be used for legged robots but not for little pet-robot.

The paper [5] investigated the CBR is a one-stage reducer with a compact structure and a wide range of installation size. But it includes only CBR bearings.

Moreover, a number of scientific works are devoted to the problem of designing mechatronic satellites [6–9] and cycloidal reducers [10–12].

Therefore, it is relevant to design an ultra-lightweight and compact cycloidal reducer.

3 Research Methodology

3.1 Designs of electrical motor and cycloidal reducer

The cycloidal reducers have a high reduction ratio, high efficiency, high stiffness, and compact size compared to conventional reduction gears, so they are attractive candidates for tight spaces and precise applications such as small pet simulated four-legged robots. Therefore, it is essential to design a device consisting of a modern mini brushless direct current electrical motor and very short sizes stage single-reducer available to operate together with the output motor shaft (Figure 1).

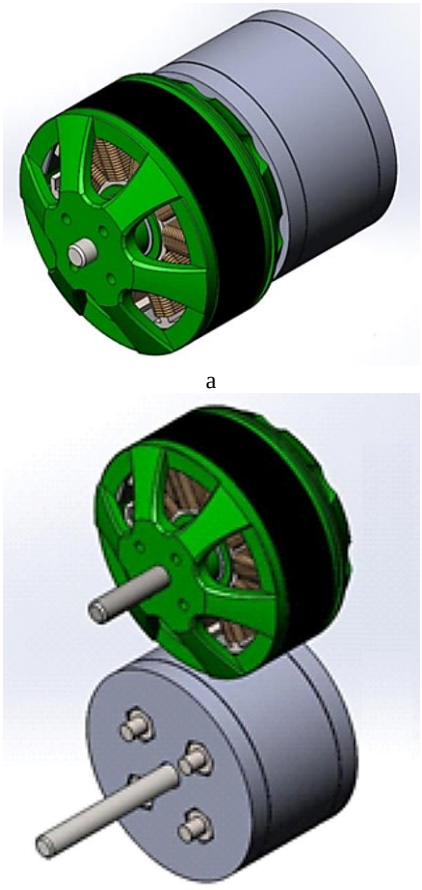

a

b

Figure 1 – Assembly of the BLDC electrical motor (a) and the cycloidal reducer (b)

Motor Multistar Elite 3508-268 KV Multirotor is usable for realizing it. Their weight is 78.6 g, the diameter is 41.8 mm, and the shaft diameter is 4.0 mm.

3.2 Usual cycloidal reducer

Figure 2 shows the development environment system information (SolidWorks) about the cycloidal disk designed by the authors.

On the diagram (Figure 2) and the reducer exploded view (Figure 3), numbers indicate the following parts: 1 – brushless DC electric motor; 2, 9 – carriers; 3, 11 – output bearings; 4, 14 – cycloidal disk bearings; 5, 15 – cycloidal disks; 6 – input shaft (crank or eccentric shaft); 7, 17 – crank bearings; 8 – bolts; 10 – slow speed shaft rollers (four pieces); 12 – internal pins wheel (output slow speed shaft); 13, 16 – bushings; 18 – four nuts (for screws and motor-reducer connecting).

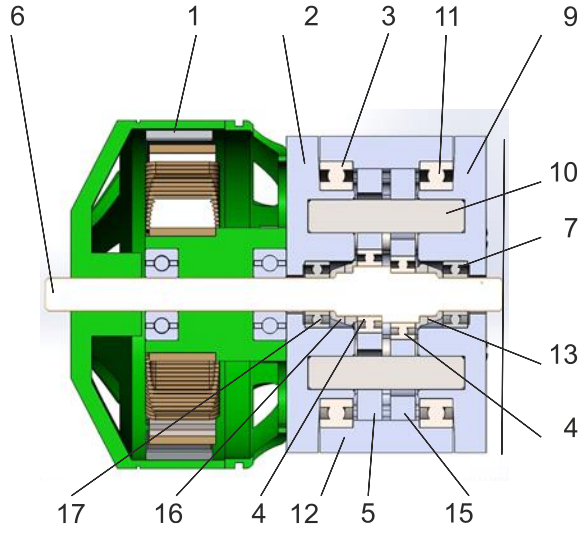

Figure 2 – Assembly axial-section sketch of the BLDC electrical motor and cycloidal reducer developed

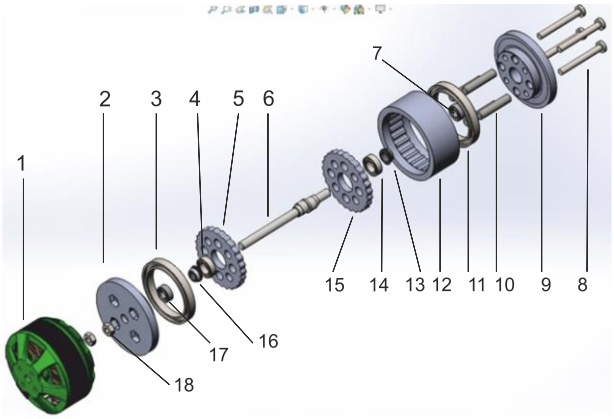

Figure 3 – Exploded view of the usual cycloidal reducer

Detailed development every of ones permit to receive their small sizes and compact assembly of reducer model design as a result.

The assembly allows putting the final design of the compact device. The essential data determined by this are the major diameter, length, and weight of the reducer. The model includes two equal cycloidal disks: parts 5 and 15, because it minimizes the vibration and improves the gear's wear resistance (Figure 3).

3.3 Minimized cycloidal reducer

Figure 4 shows the development environment system information (SolidWorks) about cycloidal disk major diameter of 32 mm.

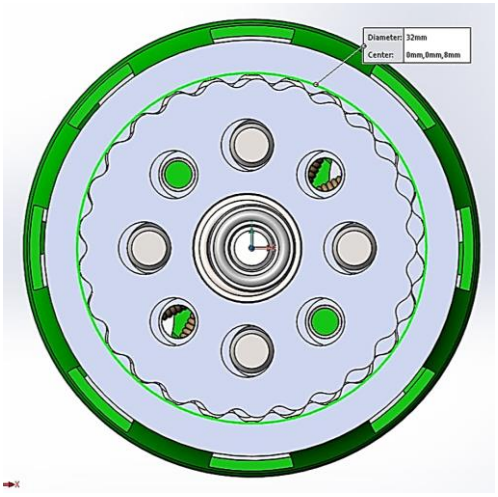

Figure 4 – Assembly cross-section sketch of the compact cycloidal reducer developed by authors

One of the essential dimensions of the reducer is the outer diameter of 38 mm (Figure 5).

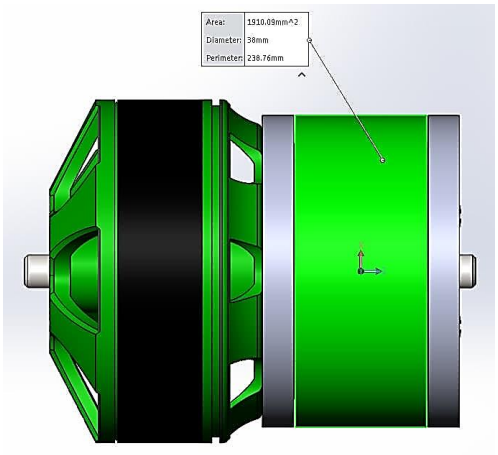

Figure 5 – Assembly drawing plan of the BLDC electrical motor and very compact cycloidal reducer developed by authors

This cycloidal reducer model predicts that the weight will not exceed 350 g if the device is made of steel parts and not more than 120 g if its biggest parts are made of plastic.

3.4 High-efficiency compact cycloidal reducer for a pet robot

It is essential to consider this value to calculate the number of cycloidal teeth and slow-speed shaft rollers.

This compact reducer includes more shaft rollers than before. There are ten rollers in its design (Figure 7). Therefore, the cycloidal disks include ten holes (Figures 7, 8).

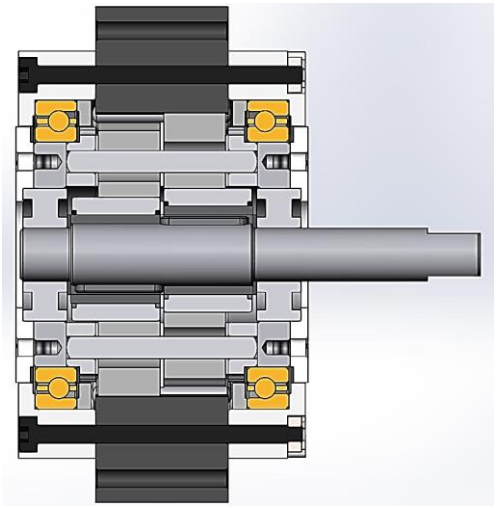

Figure 6 – View of assembly cross-section sketch of the high-efficiency compact cycloidal reducer developed by authors

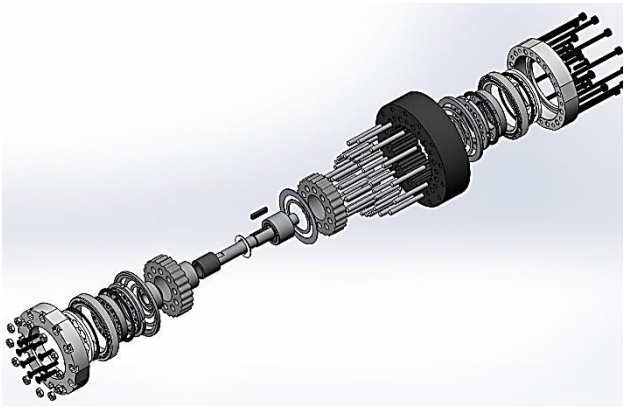

Figure 7 – Exploded view of the high-efficiency very compact cycloidal reducer developed by authors

Parameters of a reducer consider elements intended for fastening a reducer to a robot frame (Table 1).

Table 1 – Reducer parameters

Parameter	Value	Dimension
Mass	189.5	g
Diameter	56	mm
Length	41	mm
Ratio	26	–

The input shaft of the reducer is made from steel. One of the essential reducers is cycloidal disks made from plastic and slow-speed shaft rollers made from steel. Therefore, it is necessary to research the interaction between them. So the aim of the study is to receive the analysis of the stress state in a contact zone between cycloidal disks and slow-speed shaft rollers (Figure 8).

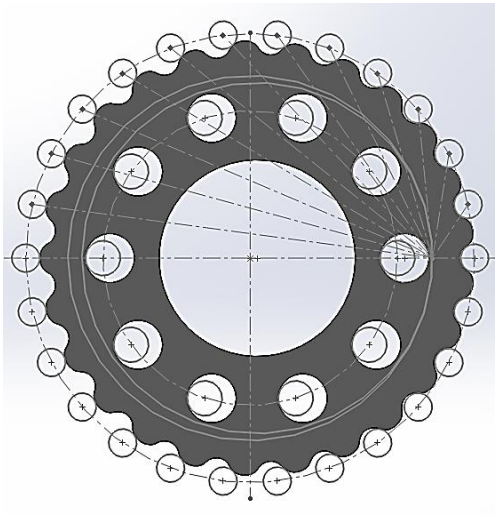

Figure 8 – Schema of interaction between cycloidal disk and slow speed shaft rollers

3.5 Computational model

Since the forces acting on the cycloid disk have a complex configuration, it is necessary to use the finite element method to determine the stresses in this part.

The stress in rollers is also easier to determine with this method due to the static uncertainty of the ones.

To speed up the calculations, simplification of the model is needed. For this reason, holes, chamfers and fillets that do not affect the result were removed. Bearings and rigid clamps were replaced with the appropriate restrictions.

Figure 9 with green arrows shows the rigid clamp, which replaced the press-fit in the carrier. The blue cones show the surfaces to which the bearing restriction has been applied.

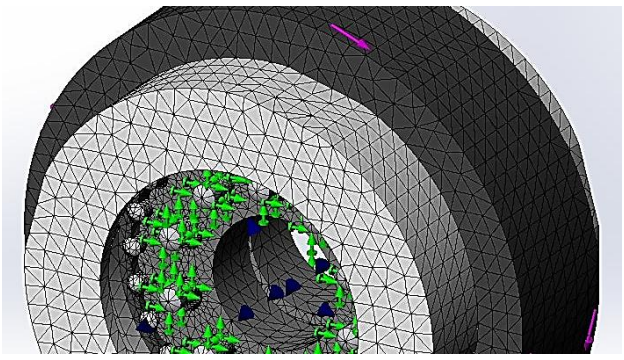

Figure 9 – applied FEM to reducer assembly

To increase the accuracy of the result, grid control was used by selecting the surfaces on which the stresses are to be determined and setting the dimensions of the grid elements on them, the sides of which are 0.5 mm. For the rest of the parts, a grid was used, the dimensions of which depend on the curvature of the surfaces with the largest elements, the dimensions of the sides of which are 2 mm.

The total number of nodes is $3.1 \cdot 10^5$. The number of elements is $2.0 \cdot 10^5$. The number of Jacobian points is 4. Solver – FFEPlus.

The contact "node to the surface" is used for the parts between which the engagement occurs. This is because the contact between the cycloid disk and the rollers looks like a line. This type of contact is better suited for such part engagement (Figure 10).

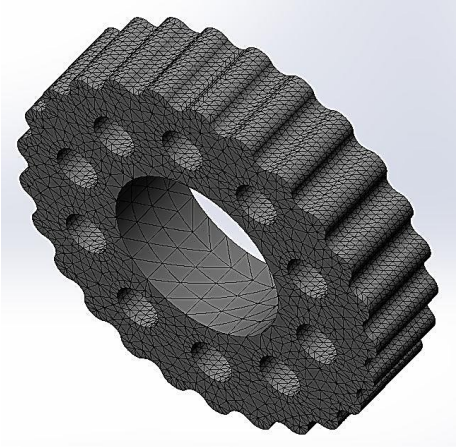

Figure 10 – Cycloid disk with FEM grid control appiled

The output link of the gearbox was loaded with a torque of 28 N·m. In Figure 9, the moment is shown by purple arrows.

The materials are selected from the SolidWorks Simulation material libraries (Tables 2, 3).

Table 2 – Characteristics of caprolon (PA Type 6) – a material selected for cycloidal disks

Property	Value	Dimension
Yield strength	108.65	MPa
Density	1120	kg/m^3
Elastic modulus	2620	MPa
Shear modulus	970.4	MPa
Poisson's ratio	0.34	–
Tensile strength	90	MPa

Table 3 – Characteristics of steel SP15 - a material selected for slow speed shaft rollers disks

Property	Value	Dimension
Yield strength	390	MPa
Density	7812	kg/m^3
Elastic modulus	$2.1 \cdot 10^5$	MPa
Shear modulus	$0.8 \cdot 10^5$	MPa
Poisson's ratio	0.31	–
Tensile strength	595	MPa

Slow speed shaft rollers with applied FEM grid control are presented in Figure 11.

Figure 11 – Slow speed shaft rollers
with FEM grid control applied

4 Results

The diagrams of the stresses in the rollers in cross section next to the satellite are shown at the base of the rollers. Stresses are caused by the reaction of the torque (Figures 12, 13).

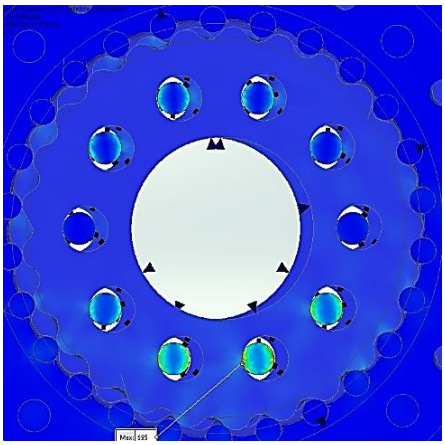

Figure 12 – Diagram of stress distribution
in slow-speed shaft rollers

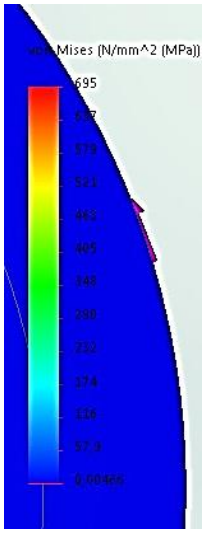

Figure 13 – The legend of the equivalent stress distribution
in slow-speed shaft rollers (von Mises)

The maximum value is 695 MPa. The strength limit for steel SH15, from which the rollers are made, is 2160 MPa.

Figures 14 and 15 show the stress diagrams of the cycloid disk.

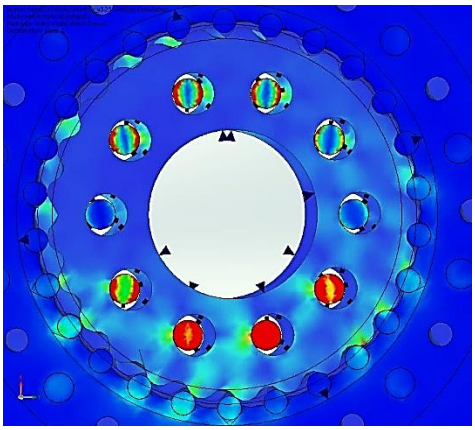

Figure 14 – Diagram of stress distribution in cycloidal disk

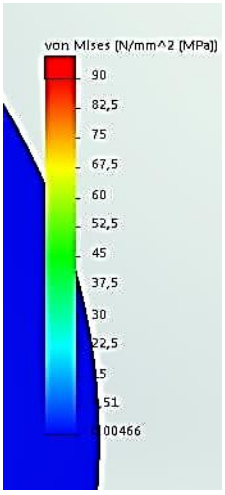

Figure 15 – The legend of equivalent stress distribution
in cycloidal disk (von Mises)

Tensile stress for graphite's saturated polyamide is 75 MPa, with relative compression strain of 135 MPa.

The maximum stress in the cycloid disk is about 90 MPa. It occurs in contact with the most loaded rollers near the surface, it is the compressive stress.

The offset of the point lying on the surface at a distance of 0.391 mm of the reducer on a radius of 28 mm is 0.8° (Figures 16).

The cycloid type of engagement selected for the stepper robot reducer allows you to design a compact and lightweight engine capable of withstanding relatively heavy loads.

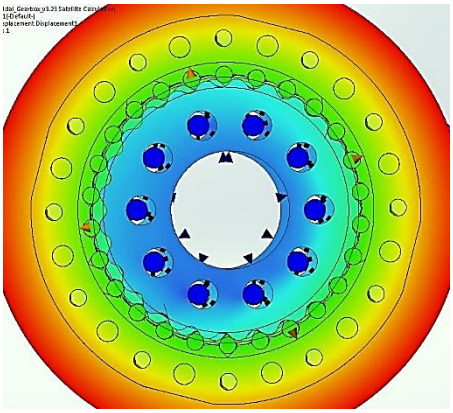

Figure 16 – Deformation diagram in a zone of the cycloidal disk

5 Conclusions

The Diameter and Length of the developed cycloidal reducer are small enough and correct to use with modern BLDC electrical motors.

The predicted weight of the developed cycloidal reducer is 180 g only.

The lightweight and compact cycloidal reducer model is developed and can be suggested as a drive for a pet simulated four-legged robot.

The obtained results of the analysis of stresses arising between the disk and the rollers indicate the complete suitability of the selected materials of polyamide and steel on their mechanical characteristics for use in the reducer of the robot activator.

Analysis of the predicted deformation of the disk demonstrates the need to use an output shaft position sensor to ensure high accuracy in determining the robot's position.

References

1. Bednarczyk, S. (2021). Analysis of the cycloidal reducer output mechanism while taking into account machining deviations. *Proceedings of the Institution of Mechanical Engineers, Part C: Journal of Mechanical Engineering Science*, Vol. 235(23), pp. 7299-7313, doi: 10.1177/09544062211016889.
2. Jung, T., Lim, J., Bae, H., Lee, K. K., Joe, H.-M., Oh, J.-H. (2018). Development of the humanoid disaster response platform DRC-HUBO+. *IEEE Transactions on Robotics*, Vol. 34(1), pp. 1-17, doi: 10.1109/TRO.2017.2776287.
3. Sensinger, J. W., Lipsey, J. H. (2012). Cycloid vs. harmonic drives for use in high ratio, single stage robotic transmissions. *The International Conference on Robotics and Automation*, Vol. 606(11), pp. 4130-4135.
4. Lee, K. K., Hong, S., Oh, J.-H. (2020). Development of a lightweight and high-efficiency compact cycloidal reducer for legged robot. *International Journal of Precision Engineering and Manufacturing*, Vol. 21, pp. 415-425.
5. Sun, X. X., Han, L. (2019). A new numerical force analysis method of CBR reducer with tooth modification. *Journal of Physics: Conference Series*, Vol. 1187, 032053, doi: 10.1088/1742-6596/1187/3/032053.
6. Qi, M., Wu, D., Zhang, S., Yao, R., Zhang, P., Han, T., Chang, J. (2018). Structural design and development of a mechatronic flywheel for miniature satellites. *Advances in the Astronautical Sciences*, Vol. 165, pp. 2219-2228.
7. Rasouli, K., Shahbazi, H., Ariaei, A., Malekzadeh, M. (2017). Mechatronic design and construction of a five axes satellite simulator. *4th RSI International Conference on Robotics and Mechatronics, ICRoM 2016*, pp. 210-215, doi: 10.1109/ICRoM.2016.
8. Li, R., Guo, F., Yu, C., He, Y., Ye, Z., Yuan, S. (2017). Development and validation of a mechatronic solar array drive assembly for mini/micro-satellites. *Acta Astronautica*, Vol. 134, pp. 54-64, doi: 10.1016/j.actaastro.2017.01.047.
9. Mendoza-Bárcenas, M. A., Vicente-Vivas, E., Rodríguez-Cortés, H. (2014). Mechatronic design, dynamic modeling and results of a satellite flight simulator for experimental validation of satellite attitude determination and control schemes in 3-axis. *Journal of Applied Research and Technology*, Vol. 12(3), pp. 370-383, doi: 10.1016/S1665-6423(14)71619-0.
10. Xie, F., Li, L., Zhang, G., Hu, X. (2021). Application of cycloidal pin wheel planetary reducer in the design of digging machine. *2021 International Conference on Electronics, Circuits and Information Engineering, ECIE 2021*, pp. 153-156, doi: 10.1109/ECIE52353.2021.00039.
11. Kormin, T. G., Tsumbu, J.-D. B. (2020). Cycloidal reducer with rotation external ring gear. *IOP Conference Series: Materials Science and Engineering*, Vol. 971(4), doi: 10.1088/1757-899X/971/4/042072.
12. Huang, J.-T., Li, C.-W. (2020). The high-payload manipulator development based on novel two-stage cycloidal speed reducers and hub motors. *Journal of Physics: Conference Series*, Vol. 1583(1), doi: 10.1088/1742-6596/1583/1/012002.